SMAR 2019 – Fifth Conference on Smart Monitoring,
Assessment and Rehabilitation of Civil Structures

SMAR 2019

Repairing and strengthening steel-corroded RC members using the cathodic protection and by mounting a stainless steel rebar

Akihisa KAMIHARAKO [1], Syuhei SASAMORI [1], Tsubasa MIURA [1], Atsushi KASHIMA [2], Yosuke KONDO [3]

[1] Hirosaki University, Hirosaki, Aomori, Japan

[2] Sumitomo Osaka Cement Co., Ltd, Tokyo, Japan

[3] Aichi Steel Corporation, Tokai, Aichi, Japan

Contact e-mail: kami@hirosaki-u.ac.jp

ABSTRACT: This study proposes a construction method for simultaneously repairing and strengthening reinforced concrete (RC) members that have been deteriorated by steel rebar corrosion via in the smallest procedure. In preparation for the tests, the main reinforcement of the RC beam was corroded using an electrolytic corrosion method. Then, the deteriorated RC beams were repaired using the cathodic protection method, which supplies power to the titanium ribbon mesh mounted into the near-surface of the groove. Afterwards, the beams were strengthened by mounting a stainless steel rebar in the groove, and a corrosion protection current was applied to the specimens. All the specimens were subjected to a loading test and their flexural behaviors were analyzed. Even when the damaged cover concrete was not repaired, the electricity behavior and structural performance of the specimens were not severely affected.

1 INTRODUCTION

In general, reinforced concrete (RC) structures with corroded steel reinforcement are repaired through patch sectioning. Then, the repaired structure is strengthened by mounting healthy steel rebars, which recover the structural performance. To enhance the strengthening effect, thedeteriorated structure is externally bonded to a steel plate, a fiber reinforced polymer (FRP) sheet, or some similar structures. In this approach, the constructer must repair and strengthen the deteriorated structure separately to improve its structural performance.

To repair and strengthen an RC member, the authors have studied the cathodic protection method and simultaneous mounting with an FRP rod (Kamiharako et al., 2016). In these studies, the FRP rod was mounted by the near-surface mounting method, which is commonly used in construction (mainly in North America) (Parvin et al., 2016). First, a groove was dug into the surface of the concrete structure as shown in Figure 1. Into this groove, the anode materials of the cathodic protection and the corrosion-resistant rebars were mounted simultaneously. In the authors' previous construction, the FRP rod was served as a corrosion-resistant rebar, which improved the flexural capacity but not the strengthening. To avoid brittle failure, a new construction method is required. Moreover, in the previous experiment on cathodic protection, the authors were only able to apply the energizing electricity for a short time. This report verifies the flexural load property of RC specimens mounted using stainless steel rebars, and the mechanical properties when sufficient electricity time was secured to resolve the above-mentioned problem.

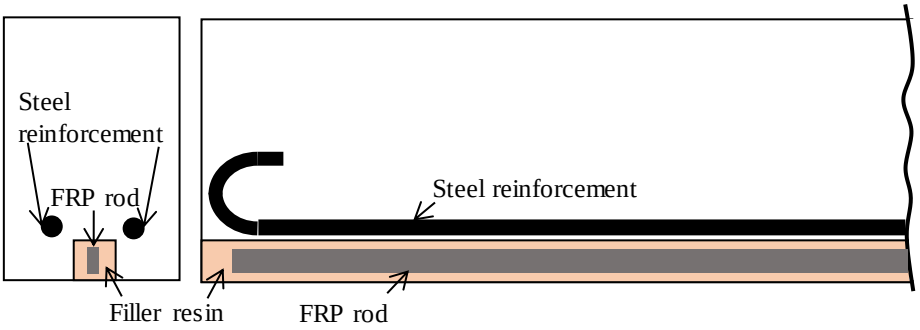

Figure 1. Example of the near-surface mounted (NSM) method of repairing deteriorated reinforced concrete structures

Step 1: Fabricate eight specimens	Step2: Conducting the electrolytic corrosion test about seven of eight specimens	Step 3: Carry out the cathodic protection test for repaired six specimens for 20 days
Step 4: Repairing and strengthening to six specimens which conducted the electrolytic corrosion test		Step 5: Conducting the flexural loading test for all eight specimens

Figure 2. Outline of this study

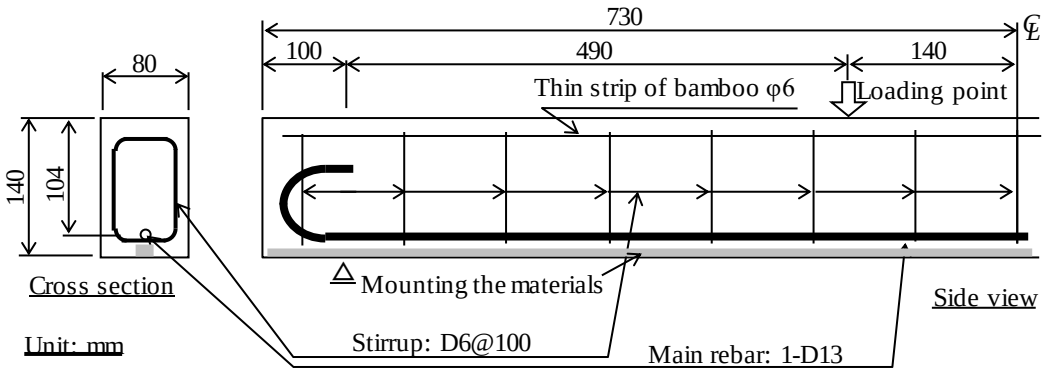

Figure 3. Schematic of RC specimen

2 OUT LINE OF EXPERIMENT

Figure 2 is a flow diagram of the present study. The contents of the experiments are explained below.

2.1 RC beams

The RC beams fabricated in this study are schematized in Figure 3. The shape and dimensions of the beam conformed to the specifications of the round robin test (JSCE, 2006). One main rebar was set at a predetermined position. The stirrups were coated with vinyl tape to avoid electrolytic corrosion. Tables 1 and 2 show the mechanical properties of the steel reinforcement and the mix proportions of the concrete constituents, respectively. In this concrete, the target

slump is 120 mm, and the target air amount is 5%. The compressive strength, measured at the end of the flexural loading test, was 33.6 N/mm^2.

The details of the specimens are given in Table 3. The length of the mounted stainless steel rebar was varied, and the deteriorated covering concrete was either repaired or not repaired. In Table 3, specimen No. 1 is the control with no corrosion, no repair and no strengthening, and specimen No. 2 was deteriorated by steel corrosion, but neither repaired nor strengthened.

Table 1. Mechanical properties of the rebars

Kind of rebar	Young's modulus (kN/mm^2)	Yield strength (N/mm^2)	Tensile strength (N/mm^2)
Stirrup: D6	190	358	597
Main rebar: D13	191	385	566
Stainless rebar: D6	158	342	713

Table 2. Admixture of concrete

W/C (%)	S/a (%)	Unit weight (kg/m^3)				
		Water	Cement	Sand	Gravel	Super plasticizer
65	40.6	158	240	778	1160	0.0204

W/C: Water to cement ratio, S/a: Sand by aggregate ratio

Table 3. List of specimens

Specimen	Main rebar corrosion	Repairing cover concrete	Mounted length of stainless rebar (mm)	Corrosion mass loss ratio of main rebar (%)	Remarks
No.1	No	N/A	–	–	Control
No.2	Yes	No	–	17.3	*
No.3	Yes	Yes	550	16.6	
No.4	Yes	Yes	825	17.1	
No.5	Yes	Yes	1100	17.9	
No.6	Yes	No	550	16.7	
No.7	Yes	No	825	17.6	
No.8	Yes	No	1100	17.4	

*: No repairing and strengthening

2.2 Electrolytic corrosion test

Specimens 2–8 were subjected to the electrolytic corrosion test. The details of this test are shown in Figure 4. The electric current for steel corrosion was provided by a stabilized DC power supply. Only the main rebar was corroded. The electricity application time for the targeted corrosion mass-loss ratio (20%) was calculated by Equation (1):

$$W = 0.866\, I_h, \tag{1}$$

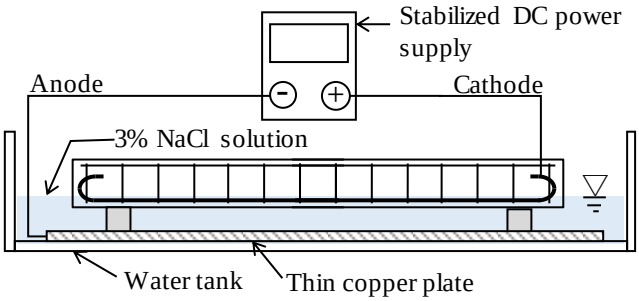

Figure 4. Schematic of electrolytic corrosion test

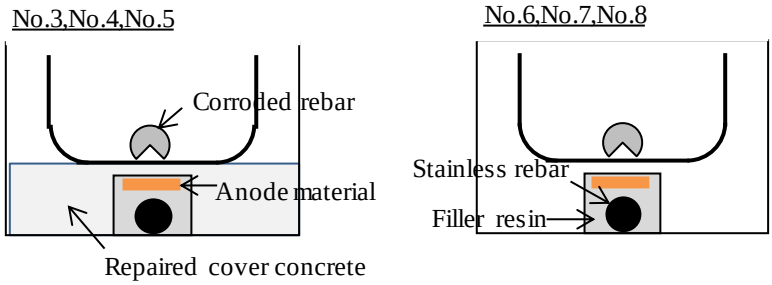

Figure 5. Schematic of repairing and strengthening

Table 4. Property of section repair material

Water-material ratio (%)	Compressive strength (N/mm^2)	
	3 days	28 days
14.5	25	45

Where W is the corrosion mass loss (grams) and I_h is the time-integrated current (ampere-hour). This expression is the empirical formula determined in previous experiments in our laboratory (e. g. Kamiharako et al., 2016). After the flexural loading test, all corroded mail rebars were excavated using an electric hummer. After removing the corroded product, the corrosion mass-loss ratio of the main rebar was measured, and the diameter reduction of the corroded rebar was measured at 25-mm intervals along the rebar by a digital vernier caliper. The corrosion mass loss ratio, C was calculated by Equation (2):

$$C = \frac{W_{cont} - W_{corr}}{W_{cont}} \quad (2)$$

Where, W_{cont} is the mass of non-corroded reinforcement and W_{cont} is the mass of corroded reinforcement.

2.3 Repairing and strengthening

The six electrolytically corroded specimens were repaired by the cathodic protection method, and strengthened by mounting a stainless steel rebar. Figure 5 presents schematics of the RC beam sections after repairing and/or strengthening. As shown in Table 3, the repairing and strengthening procedures were performed or not performed on individual specimens. In Specimens 3–5, the damaged cover concrete was removed by a static crush agent with a slow

expansion property, which eventually crushed the concrete. Afterwards, the RC beam was installed in the form used at the time of beam casting, with the main rebar at the top. In this state, the form was filled with high-flow patch repair mortar to repair the damaged cover concrete. The compressive strength property of high-flow mortar is shown in Table 4. A groove of width 20 mm and depth 25 mm was dug along the full length of the RC beam with a concrete cutter. The anode materials were laid in the groove and coated by backfilling the groove with mortar. The anode material was titanium ribbon mesh with dimensions of 12.7 mm × 1,500 mm × 0.635 mm (width × length × thickness), and a lengthwise resistance of 0.37 Ω/m. After curing for 3 days, the stainless steel rebar was inserted in the groove and filled with the same mortar.

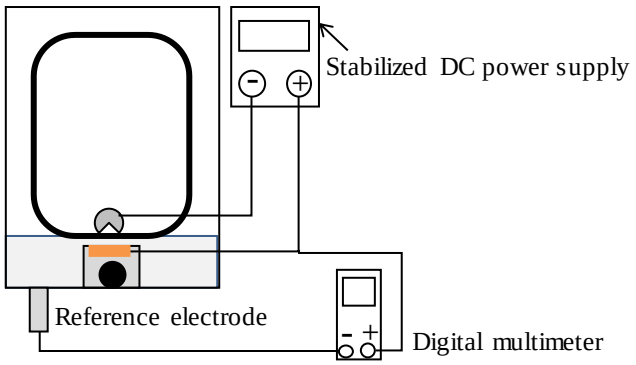

Figure 6. Schematic of cathodic protection test

2.4 Cathodic protection test

The impressed current system used in the cathodic protection test is shown in Figure 6. The six experimental RC beams were divided into three groups and connected in series with a stabilized DC power supply, which supplied the protection current to the specimens. During energizing by the current, the instant off/on potential was measured daily by a lead reference electrode and a digital multimeter. The depolarization value of the main rebar was calculated as the instant off or on potential, and the protection current to the specimens was applied for approximately 20 days. The instant on/off potential was measured at two points located 490 mm inward from each beam end. The current density for the main rebar, determined in a polarization test, was 6.9 mA/m^2. This value was constant during the cathodic protection test.

2.5 Flexural loading test

After repairing, strengthening, and cathodic protection, all specimens were subjected to flexural loading tests. The locations of the loading and support points are shown in Figure 3. The bending test was conducted at four points to ensure a uniform bending-moment section. During the loading test, the applied load and deflection at the mid-span were measured by a data acquisition system.

3 TEST RESULTS AND DISCUSSION

3.1 Corrosion mass loss of main rebar

The average corrosion mass-loss ratios of the rebars in the specimens are listed in Table 2. Figure 7 shows the longitudinal distributions of the diameter reduction along the corroded rebars. The average mass-loss ratio almost reached the target value of 20%, indicating the success of the electrolytic corrosion test. Also, the diameter-reduction distributions exhibited no extreme deflections. Therefore, the corrosion property in each test specimen was assumed to be approximately equal.

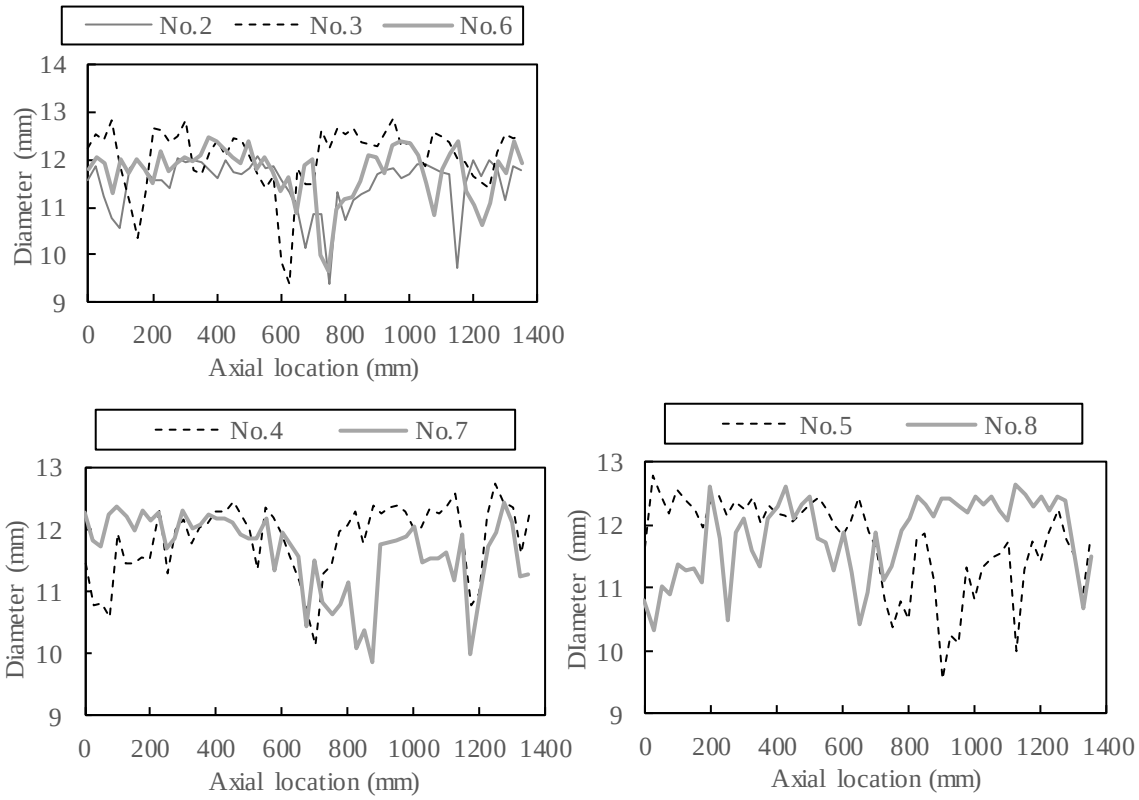

Figure 7. The longitudinal distribution of the decreased diameter

3.2 Cathodic protection test

Figure 8 plots the depolarization values in specimens 3–5 (left panel) and 6–8 (right panel) as functions of elapsed time. The plotted values are the means of the measurements at the two designated points. The current provided to all specimens exceeded 100 mA, the protection standard in Japan (JEA, 2012). The protection effect was high in the specimens with the unrepaired concrete cover, but (as evidenced by the low depolarization) low in the repaired specimens. Therefore, the cover-concrete repair did not provide a desirable protection effect. This result is probably related to the higher hydrous state of the repaired cover concrete than of the unrepaired concrete. Such a difference in the hydrous state may influence the current energization situation.

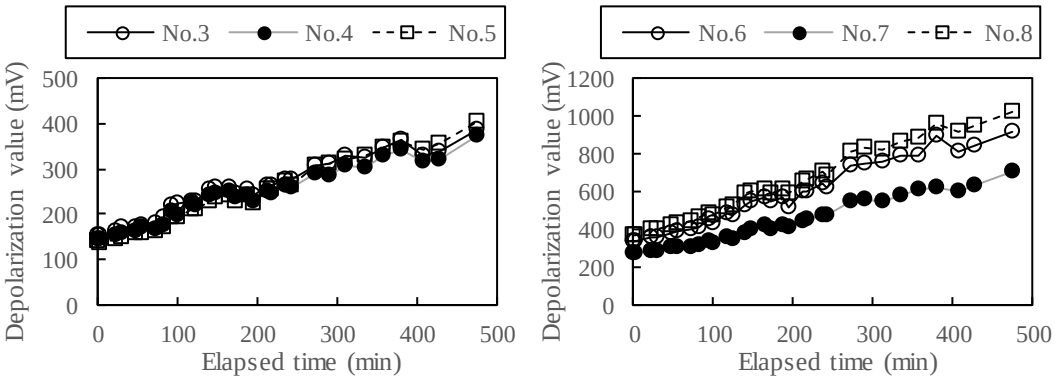

Figure 8. The relationships between depolarization value and elapsed time

3.3 Flexural loading test

The relationships between load and deflection at mid-span for groups of specimens are shown in Figure 9. When the mounted stainless steel rebar was relatively short (550 mm), brittle-like failure occurred because of bond splitting failure in the rebar. However, when the mounted stainless steel rebar was relatively long, the load–deflection curves exhibited ductile behavior, regardless of whether the cover concrete was repaired or not. Therefore, the repair procedure did not greatly influence the structural performance of the specimens (although the result is reported for completeness).

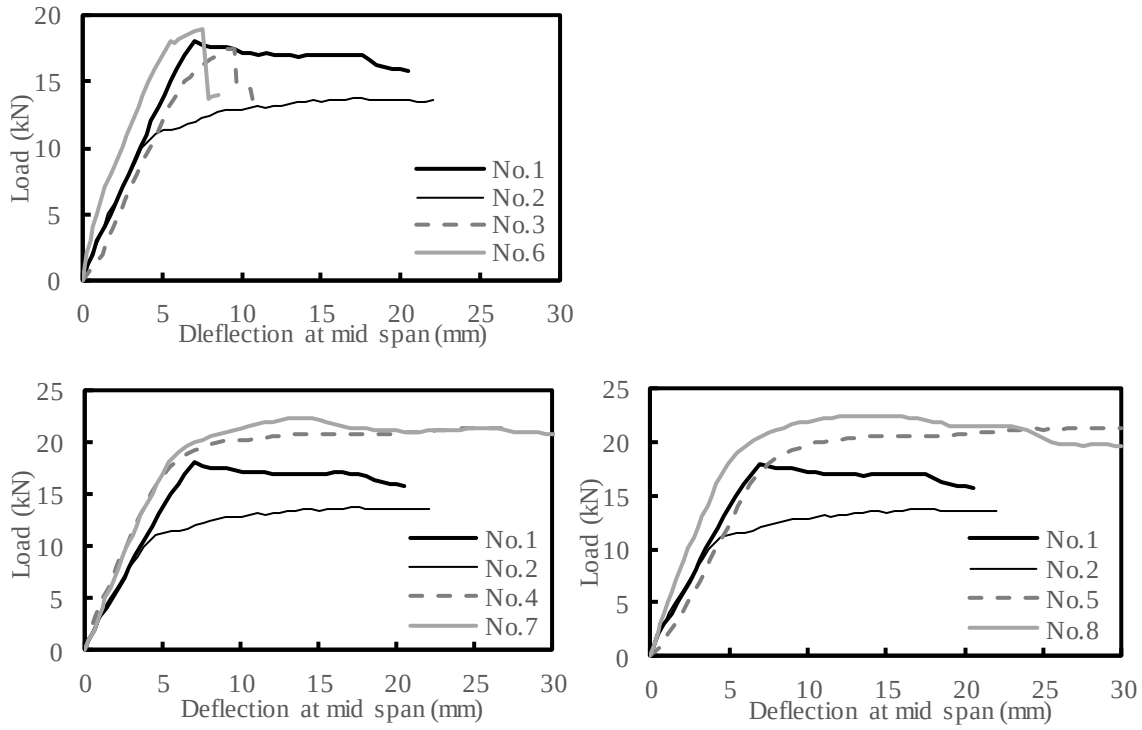

Figure 9. The relationships between load and deflection at mid span

4 CONCLUSION AND REMARKS

The conclusions of the study are summarized below.

This study investigated a construction method that repairs deteriorated RC members by cathodic protection and simultaneously strengthens them by mounting a stainless steel rebar. The test results confirmed the repairing and strengthening abilities of the proposed method.

In the cathodic protection test, repairing the covering concrete reduced the depolarization value, implying that the desirable protection effect was not achieved. This poor performance was attributed to the overly hydrous state of the cover concrete.

When the mounted stainless steel rebar was relatively short, brittle-like failure was observed in the flexural loading tests. Ductile behavior was achieved by lengthening the mounted stainless steel rebar, regardless of whether the covering concrete was repaired or not.

Overall, repairing the covering concrete did not greatly influence the test results. The authors hope to validate the concrete repair procedure in future work.

ACKNOWLEDGEMENT

This research was supported by the Ministry of Education, Science, Sports and Culture, Grant-in-Aid for Scientific Research (B), 2017-2020（17H03289, Shinichi Miyazato）.

REFERENCES

Japan Society of Civil Engineers, 2009, *Structural performance of the concrete which materials deterioration*, Concrete Engineering Series, 85

Japan Elgard Association, 2012, *Cathodic Protection of Steel Reinforced Concrete*, Shinken Press, Inc.

Kamiharako, A et al, 2013, Repair and Strengthening of RC Member Damaged by Steel Corrosion and Verification of Re-deterioration Behavior, *Proceedings of Third International Conference on Sustainable Construction Materials and Technologies*, In DVD-ROM

Kamiharako, A et al, 2016, Simultaneous Construction of Repairing and Strengthening for Corroded RC beam, *The proceedings of 71th annual meeting of the Japan Society of Civil Engineers*, **V**, 771-772

Parvin and T. Syed Shah, 2016, Fiber Reinforced Polymer Strengthening of Structures by Near-Surface Mounting Method, *Polymers*, **8**, e298, https://doi.org/10.3390/polym8080298